Physics and Imaging in Radiation Oncology 27 (2023) 100470

Contents lists available at ScienceDirect

Physics and Imaging in Radiation Oncology

journal homepage: www.sciencedirect.com/journal/physics-and-imaging-in-radiation-oncology

Original Research Article

Difference between planned and delivered radiotherapy dose to the internal mammary nodes in high-risk breast cancer patients

Anders W. Mølby Nielsen [a,*], Harald Spejlborg [b], Christina Maria Lutz [b], Per Rugaard Poulsen [c,d], Birgitte Vrou Offersen [a,c,d]

[a] Department of Experimental Clinical Oncology, Aarhus University Hospital, Aarhus, Denmark
[b] Department of Medical Physics, Aarhus University Hospital, Aarhus, Denmark
[c] Danish Center for Particle Therapy, Aarhus University Hospital, Denmark
[d] Department of Oncology, Aarhus University Hospital, Aarhus, Denmark

ARTICLE INFO

Keywords:
Breast cancer
Internal mammary node irradiation
Cine MV images
Delivered dose

ABSTRACT

Background and purpose: Chest wall movement during radiotherapy can impact the delivered dose to the internal mammary nodes (IMN) in high-risk breast cancer patients. Using portal imaging and dose reconstruction we aimed to examine the delivered IMN dose coverage.

Material and methods: Cine MV images were recorded for 39 breast cancer patients treated with daily image-guided radiotherapy (IGRT) in deep-inspiration breath-hold (DIBH). On the final frame of each cine MV recording the chest wall was matched with the Digitally Reconstructed Radiograph (DRR) from the treatment plan. The geometrical chest wall error was determined in the imager-plane perpendicular to the cranio-caudal direction, rounded to integer millimeters, and binned. For each 1 mm bin, an isocenter-shifted treatment plan was recalculated assuming that the projected error observed in the cine MV image was caused by anterior-posterior chest wall movement in the IMN region. A weighted plan sum yielded the IMN clinical target volume receiving at least 90% dose (V90_CTVn_IMN).

Results: The mean number of cine MV observations per patient was 36 (range 26–55). Most patients (67%) had on average a posterior chest wall position at treatment compared to planned. This translated into a change in the delivered median V90_CTVn_IMN of −0.7% (range, −11.9–2.9%; $p < 0.001$). The V90_CTVn_IMN reduction was greater than 9% in three patients. No clinically relevant differences were found for the mean lung dose or mean heart dose.

Conclusion: Using cine MV images, we found that the delivered V90_CTVn_IMN was significantly lower than planned. In 8% of the patients, the V90_CTVn_IMN reduction exceeded 9%.

1. Introduction

Internal mammary node irradiation (IMNI) in high-risk breast cancer (BC) patients reduces distant recurrence, BC specific mortality [1–3] and improves overall survival [3]. However, IMNI may increase the risk of ischemic heart disease. In early BC studies, excess cardiac disease [4] and mortality were observed in left-sided BC patients [5], and a dose–response relationship between mean heart dose (MHD) and major coronary events was established in 2D-based radiotherapy (RT) [6]. In a modern cohort of BC patients treated with tangential 3D-CT RT, the risk of cardiac events diagnosed with invasive procedures was not increased within 10 years after RT in left-sided patients [7].

However, the transition from 2D-based RT to tangential 3D-CT RT caused a slight decrease in IMNI target coverage [8,9]. Planning IMNI is often a balance between target coverage and constraints to organs at risk (OAR). A treatment planning study has shown that, despite employing steep dose gradients, it was not possible to achieve full IMN dose coverage while keeping OAR constraints in a subgroup of patients [10]. A recent study found a low median MHD (1.6 Gy) in left-sided BC patients, though different dose distributions were shown across centers, indicating that the balance between target coverage and OAR sparing was prioritized differently across centers [11]. Hence, IMNI may be particularly sensitive to setup errors including internal movement during treatment.

* Corresponding author at: Department of Experimental Clinical Oncology, Aarhus University Hospital, Palle Juul-Jensens Boulevard 99, 8200 Aarhus N, Denmark.
E-mail address: awmnielsen@oncology.au.dk (A.W.M. Nielsen).

https://doi.org/10.1016/j.phro.2023.100470
Received 2 May 2023; Received in revised form 5 July 2023; Accepted 6 July 2023
Available online 12 July 2023

Deep inspiration breath hold (DIBH) can increase the distance between BC target structures and the heart. The DIBH gating level is often monitored by an external marker block on the chest wall [12]. The marker block position is, however, only a surrogate of the real internal chest wall movement. The internal chest wall position during treatment can be obtained by continuous portal imaging (cine MV) of tangential field delivery [13,14]. By this means, the mean chest wall position in gated BC patients deviated only 0.1 mm from planned [13]. However, in 2.2% of the recorded fields the error was above 5 mm, and in 43% of the patients, the intra-field chest wall movement range exceeded the external gating window, highlighting that the external marker block movement may not in all patients represent the internal chest wall movement [13,15]. A possible pitfall is a caudal marker block placement on the thoracic wall, which has shown a worse correlation with chest wall position compared to mid-sternal and cranial placement [16]. In other studies, a systematic posterior movement of the target was observed during treatment delivery [17] or even already during the setup procedure [18]. Hypotheses to explain this phenomenon include relaxation [18] and fatigue during treatment [19]. DIBH can also be monitored with spirometry or with surface guidance (SGRT), though these methods have not been shown to further improve chest wall stability [20–22].

Only a few studies have used intrafractional geometrical chest wall movements to estimate delivered RT dose coverages. The impact of the observed intrafractional chest wall movements on the delivered doses to OARs and the breast target was found negligible [15,23]. However, to the best of our knowledge, no studies have used Cine MV images to investigate the actual delivered IMNI dose.

Therefore, due to the vulnerable nature of the IMN target and the existing gap in the literature, we examined the geometrical errors and the impact on IMN dose coverage during delivery of main tangential fields using cine MV images in a cohort of high-risk BC patients treated with DIBH and image-guided RT (IGRT).

2. Material and methods

2.1. Patient cohort

A prospective single-center quality assurance study was conducted in a consecutive cohort of all left-sided node-positive BC patients treated with IMNI using DIBH at Aarhus University Hospital during 2021. Patients with bilateral disease or treatment in non-supine position were excluded. In total 39 high-risk BC patients were included (supplementary material A and figure S1). The project was approved by our institutional review board.

2.2. Treatment planning

Patients were scanned and treated in DIBH, monitored and guided by Respiratory Gating for Scanners [RGSC, Varian Medical Systems, Palo Alto, Ca, USA]. Patients were immobilized in supine position in a breast board (Candor XRT) with the ipsilateral arm elevated above the head and the contralateral arm adducted alongside the chest. A marker block was placed on the lower part of the sternal bone at the junction with the xiphoid process, monitored by the RGSC system. Patients were trained at the CT session before the DIBH CT scan was acquired, and a comfortable gating level that the patient could hold for at least 20 s was found. The standard gating window was 2 mm. The slice thickness of the treatment planning CT was 3 mm. Target delineation followed the guidelines of the European Society for Radiotherapy and Oncology [24]. The CTVn_IMN included the third intercostal space (ICS) in all patients and the fourth ICS in case of a caudal and medially located tumor. For treatment planning, a single-isocenter technique was used. Two tangential fields were applied with a supplementary periclavicular field. Top-up intensity-modulated RT enhanced dose homogeneity. All treatment plans were calculated using the AcurosXB_16.1.0 calculation model (Eclipse treatment planning system, Varian). The Danish Breast Cancer Group (DBCG) recommends V90_CTVn_IMN $\geq$ 98%, and OAR constraints were MHD $\leq$ 5 Gy and mean lung dose (MLD) $\leq$ 18 Gy. A PTV margin of 5 mm to all target structures was recommended, though the PTV margin was prioritized below constraints to the heart and lungs. Hence, the PTV margin, and also sometimes the V90_CTVn_IMN, was susceptible to dose compromises. Patients were treated with either 40 Gy/15 fx or 50 Gy/25 fx. In patients with breast-conserving surgery, a tumor bed boost was given as a simultaneous integrated boost with 45.75 Gy/40 Gy/15 fx or 57 Gy/50 Gy/25 fx for patients aged 41–49 years and 52.2 Gy/42.3 Gy/18 fx or 63 Gy/51,52 Gy/28 fx for patients $\leq$ 40 years or with a tumor resection margin $<$ 2 mm.

2.3. Treatment delivery

At the treatment sessions, patients were positioned according to skin marks followed by daily IGRT including an MV image of one tangential field and a corresponding orthogonal kV image. These were matched to the treatment plan digitally reconstructed radiographs (DRR) and the patient position was corrected by couch movement before treatment. Both patient setup imaging and treatment delivery were gated in DIBH. During treatment delivery, cine MV images were recorded at every fraction for both the medial and lateral tangential fields. In the clinical setting, the cine MV images were reviewed offline by a medical physicist after the second fraction for a selection of patients (challenges in cooperation during the CT session, abdominal DIBH, field edge within 1 cm of the heart). The purpose was to detect setup errors greater than 3 mm to take counteractive action, e.g., additional gating training, repositioning of the marker block or a rescan to make a new treatment plan. Based on the 5 mm PTV margin, a 3 mm cut-off was pragmatically chosen as a compromise between negligible errors and errors with dosimetric consequences.

2.4. Geometrical errors

In the present study, the chest wall location in the final frame of each cine MV series was matched post-treatment to the corresponding DRRs from the two main tangential fields in the treatment plan. The chest wall geometrical error was measured in the imager plane perpendicular to the cranio-caudal direction (u-direction, Fig. 1). Assuming that the chest wall region closest to the CTVn_IMN was a good surrogate for the IMN position, the match was performed for this region (Fig. 1C). To account for residual match errors in the daily IGRT and couch correction procedure, also the acquired tangential setup MV image was matched with the DRR in this region closest to the IMN position (Fig. 1C). This post-treatment IMN match deviated from the daily clinical match priorities (Fig. 1B). The differences between the IMN match and the daily clinical match were attributed to pitch rotation around the right-left axis, which was furthermore evaluated visually. The difference between this residual match error and the actual error in cine MV image during treatment was ascribed to intrafractional chest wall movement from setup imaging to treatment. To explore a possible correlation between marker block positioning and IMN dose coverage, the distance from the marker block to the junction between the sternal bone and the xiphoid process was measured on the planning CT-scan (figure S2).

2.5. IMN dose reconstruction

The geometrical chest wall errors in the cine MV images were rounded to integer millimeters and binned for each treatment field observation. For each 1 mm bin, a new treatment plan was recalculated with a shifted isocenter. It was assumed that the error in the u-direction observed in the cine MV image was caused by an anterior-posterior chest wall movement in the IMN region. This allowed calculation of a weighted plan sum of the delivered CTV dose from the whole treatment course. From this, the delivered V90_CTVn_IMN was calculated and

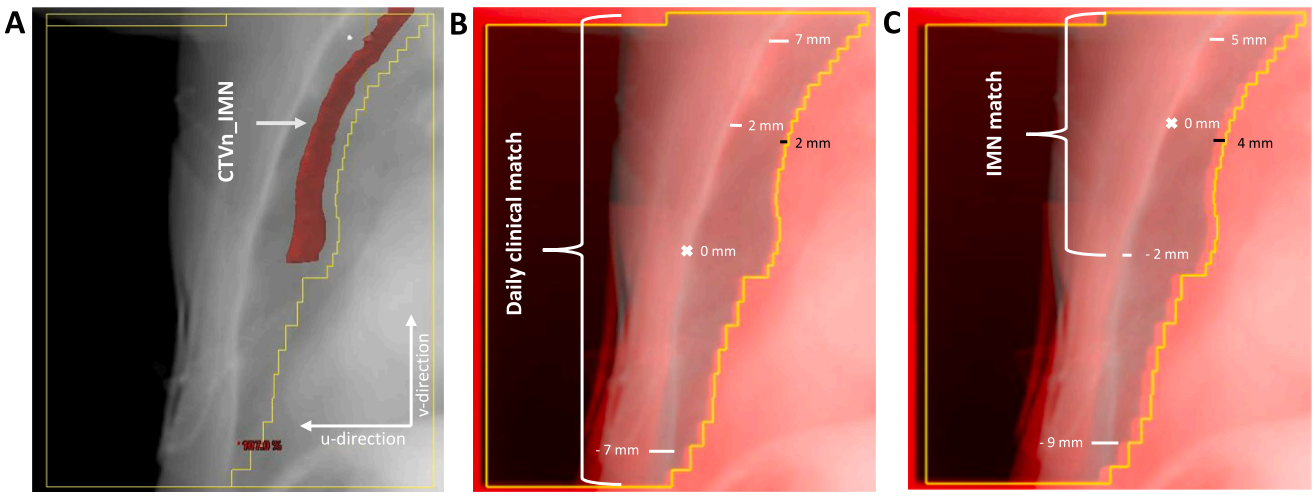

Fig. 1. A. Beams eye view of lateral tangential field 1 with overlayed IMN segmentation (red structure). The white arrows show the u-direction and the v-direction **B-C.** Blended image of a cine MV image (red) and DRR (light blue) for a fraction with a posterior pitch. The black bars show the u-directional geometrical error. **B.** Shows the residual errors applying the daily clinical match as used in the clinical setting. **C.** Shows the residual error when applying a match strategy that focuses on the IMN region. It is seen that there are residual errors in both match strategies but in different regions. Patient 34, fraction 10, field 1 has been used for Fig. 1. (For interpretation of the references to color in this figure legend, the reader is referred to the web version of this article.)

compared with the planned dose.

2.6. Statistics

The population mean error M, and the standard deviation (SD) of the systematic error $\sum$ and the random error σ in the u-direction were calculated according to van Herk [25]. Geometrical errors were also presented as simple means with 95% confidence intervals. The primary outcome was the difference between delivered and planned V90_CTVn_IMN. Differences were tested with the non-parametric signed-rank test. Pearson correlation coefficient was used to test correlation between two continuous variables. Normality of data was assessed with histograms and QQ-plots. All statistical analyses were done in Stata 17.0 (StataCorp LLC, Texas, USA).

3. Results

In the setup MV images, 46% of fractions were assessed to have no pitch, 17% to have a posterior pitch i.e., the cranial part of the thoracic wall falling more posterior than the caudal part, and 36% to have an anterior pitch. For field 1 and 2 combined, 49%, 24%, and 27% of the cine MV images were without, with a posterior, and with an anterior pitch, respectively. Matching the chest wall in the cine MV image to the DRR in the CTVn_IMN target region most patients (67%) had on average a posterior chest wall position on cine MV images compared to the planned position (Fig. 2). The geometrical error in field 1 was strongly correlated to the error in field 2. The geometrical errors combined for field 1 and 2 were according to van Herk; M = 0.7 mm, $\sum$ = 1.4 mm, and σ = 1.7 mm. In 3% of the observations the error was larger than 5 mm. Intrafraction chest wall movement was the main constituent of the geometrical error (Fig. 3D). Results for the daily clinical match method are supplied in supplementary materials B.

A posterior geometrical error entailed, in contrast to anterior errors that the IMN target moved partly out of the high-dose region (Fig. 4). This translated into a statistically significant change of the delivered median V90_CTVn_IMN of −0.7% ($p < 0.001$). The difference in V90_CTVn_IMN ranged from a 2.9% increase to an 11.0% reduction in delivered compared to planned dose. The V90_CTVn_IMN reduction was greater than 9% in three patients (Fig. 5). A dosimetric example is provided in Fig. 6. The median planned MHD was 1.3 (range: 0.5—4.5) Gy and the median estimated delivered MHD was 1.3 (range: 0.5–4.4) Gy ($p = 0.04$). The median planned MLD was 11.4 (range: 7.7–16.1) Gy and the median estimated delivered MLD was 11.3 (range: 7.3–16.6) Gy, $p = 0.007$.

In 27 of 39 patients, the cine MV images were reviewed by a medical physicist after the second fraction, but only in four patients was the cine MV review performed at more than two fractions. The median distance between the junction of the sternal bone/xiphoid process and the measuring point on the marker block was 4.4 cm (range 0.9–9.7 cm). No correlation was found between the magnitude of the marker block position in cranio-caudal direction and the field 1 error, field 2 error, or the difference between delivered and planned V90_CTVn_IMN.

4. Discussion

To our knowledge, this is the first report estimating the delivered V90_CTVn_IMN doses for BC RT. We found a statistically significant reduction of the median V90_CTVn_IMN of 0.7% with a maximum reduction of 11%. The reduction was greater than 9% in three patients. No clinically relevant differences between delivered and planned MLD and MHD were found. Both geometrical errors and a vulnerably planned V90_CTVn_IMN could explain these findings.

First, our data shows that the V90_CTVn_IMN was more vulnerable to setup errors than MLD and MHD. The sensitivity toward geometrical errors varied among patients and seemed more pronounced in patients with a low planned V90_CTVn_IMN (Figs. 4 and 5). This is caused by the steep dose gradient of IMNI on the edge of the tangential fields, which reflects the trade-off between target and OAR doses. No clinically relevant differences were found for OAR doses indicating more robustness towards the observed geometrical errors. As there is level 1 evidence supporting overall survival gain from IMNI, the CTVn_IMN needs to have priority in RT planning of high-risk BC patients [1–3]. The risk of ischemic heart disease and second lung cancer is also of concern, however, with modern RT planning according to DBCG guidelines it is unlikely that dose to these OAR influences survival at least within the first decade [7,26].

Second, impact of marker block position has previously been investigated at our institution, and acceptable chest wall position reproducibility was found for sternal bone placement of the marker block. [13]. Not in line with this, we found the marker block displaced 4.4 cm (median value) below the xiphosternal junction. This could be caused by the practical problem of placing the marker block between the breasts

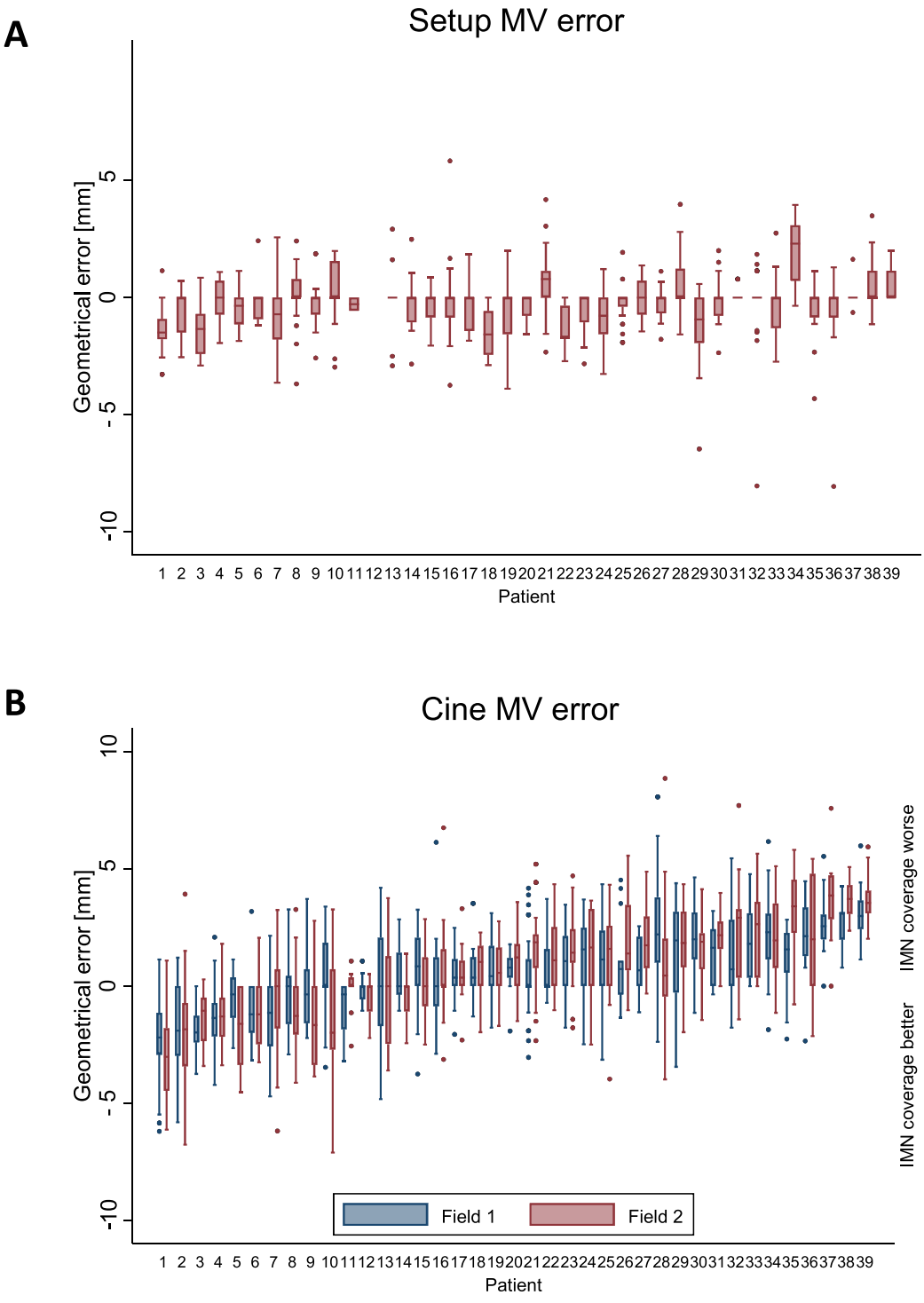

Fig. 2. Geometrical error of the chest wall in the u-direction in MV images. Patients sorted according to mean geometrical errors in field 1 and field 2 from most anterior deviation (patient 1) to most posterior deviation (patient 39). Boxplot shows the 25th and 75th percentile with a median bar in the middle. Whiskers defined as by Tukey. Outside values shown. **A.** Setup MV error after daily IGRT procedure and correction. Notice, that the median value is zero for 27 of the patients. Patient 12 was treated with cone beam CT only as daily IGRT, hence no setup MV values **B.** Cine MV error of field 1 and 2.

and the worry of introducing a bolus effect causing skin damage. We found no correlation between the magnitude of caudal displacement of the marker block from the sternal bone and reduction in delivered V90_CTVn_IMN. However, in line with previous findings [16], the general caudal displacement of the marker block toward the abdomen may contribute to the poor reproducibility of the chest wall position, since in this case abdominal movements rather than the chest wall movements are monitored by the gating system.

Third, the daily IGRT was not always representative of the chest wall position during treatment. Our data suggest this in three ways. First, the number of patients with an anterior pitch decreased from the setup MV image of daily IGRT to cine MV images of the delivered fields, in line

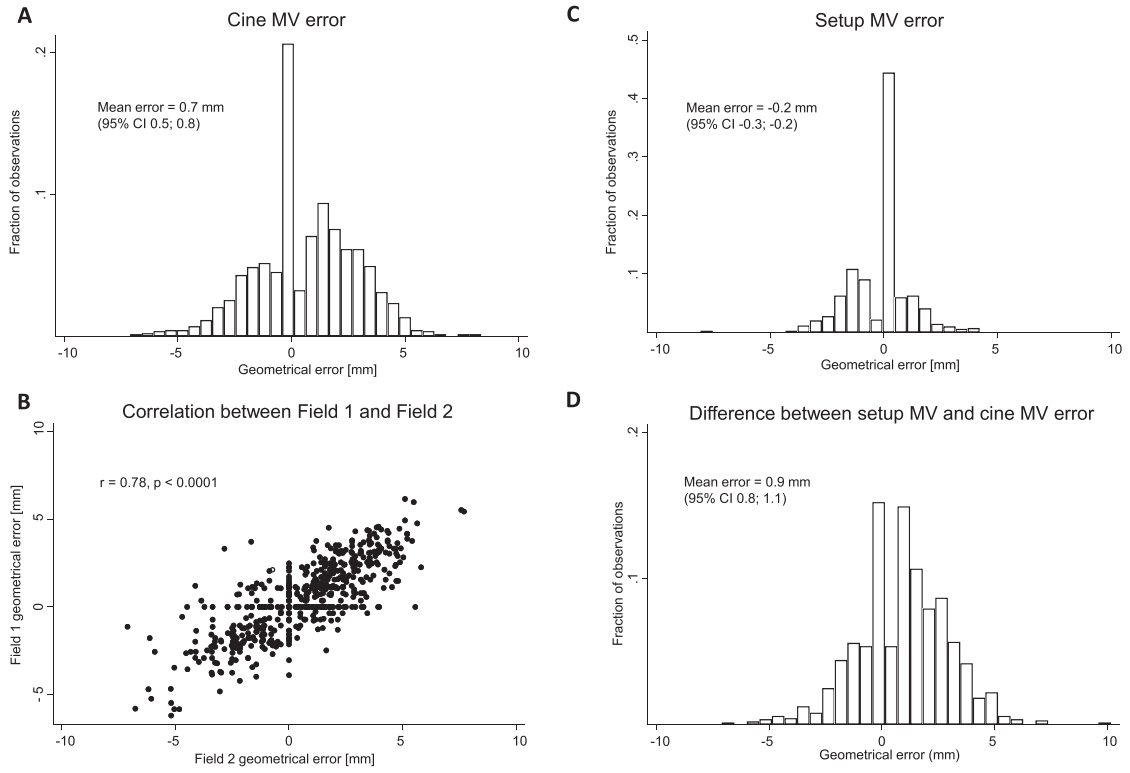

Fig. 3. **A**. Histogram of measured geometrical errors in the final frame cine MV images in the u-direction compared to the planned position. **B**. Correlation between field 1 and 2 geometrical errors. Pearson correlation coefficient shown in figure. **C**. Residual geometrical error at the setup MV image when applying the IMN match after initial couch correction. **D**. Geometrical errors originating from intrafraction chest wall movements derived as the difference between the setup MV error and the cine MV error.

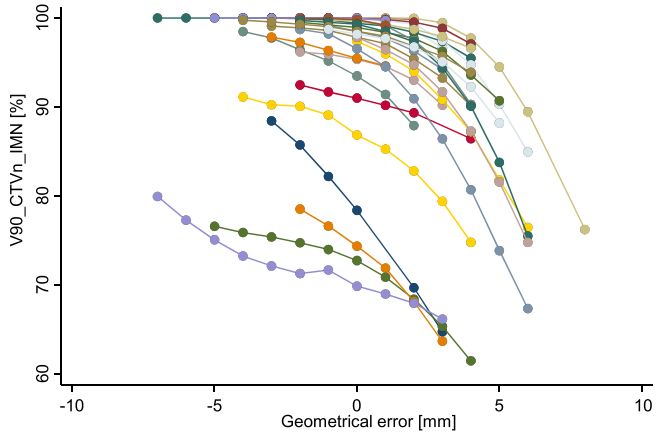

Fig. 4. Reconstructed treatment plans for each 1 mm bin. If the patient had at least one deviation in the specific bin, a recalculated treatment was reconstructed. Each colored curve represents one patient.

with the previously proposed relaxation theory [18]. Second, the geometrical errors mainly originated from intrafraction chest wall movements (Fig. 3). Third, the geometrical error was larger than 5 mm in 3% of all observations, previously estimated to 2.2% [13].

Another modality for daily IGRT is cone beam CT (CBCT). 2D portal images underestimate the bony set-up error compared with CBCT [27]. A possible advantage of CBCT is the prolonged image capturing time, which we believe is more representative of the average chest wall position during DIBH compared with the snapshot approach of 2D IGRT.

Finally, a cine check was applied after the second fraction in 67% of the patients, and follow-up checks were rarely carried out. As geometrical errors can vary over the entire course of RT, cine checks at a larger proportion of fractions, or automating the process, would likely enhance the probability of detecting patients with the largest geometrical errors.

A primary strength of our study is that it was conducted in a consecutive cohort representing a full calendar year. Unlike most research in the area, the match between cine MV images and the planned position from the DRR was done manually, and every cine MV image was reviewed twice according to the two listed match strategies by one investigator. Important limitations were the assumptions made in recalculating the treatment plans. First, we assumed the final cine MV frame to be representative for the entire field delivery, which was based on clinical experience from our institution and from Lutz et al, who described a small SD of intra-field movement of the chest wall of 0.5 mm [13]. Second, we assumed that the error observed at the chest wall in the u-direction originated solely from an anterior-posterior movement. This was found most plausible and dosimetrically valid as the observed u-error gives the same dosimetric effect on the V90_CTVn_IMN whether it originated from an anterior-posterior or medial–lateral geometrical error due to the tangential field arrangement. Third, we assumed no cranio-caudal movement as this movement is difficult to quantify accurately on cine MV images from tangential fields alone, and such movement would occur mainly along the steep dose gradients near the IMN and not perpendicular to it. Finally, we assumed no rotation or deformation. Taken together, with these simple assumptions we find our dose reconstruction provides a valid estimate of the V90_CTVn_IMN.

These results raised awareness around all factors contributing to setup errors during RT in high-risk BC patients at our department. This included focus on optimal marker block positioning (i.e. on the sternal bone), improved DIBH training, and improved daily IGRT by implementing CBCT. Prioritizing a PTV margin above constraints to OAR would be another way to improve V90_CTVn_IMN coverage.

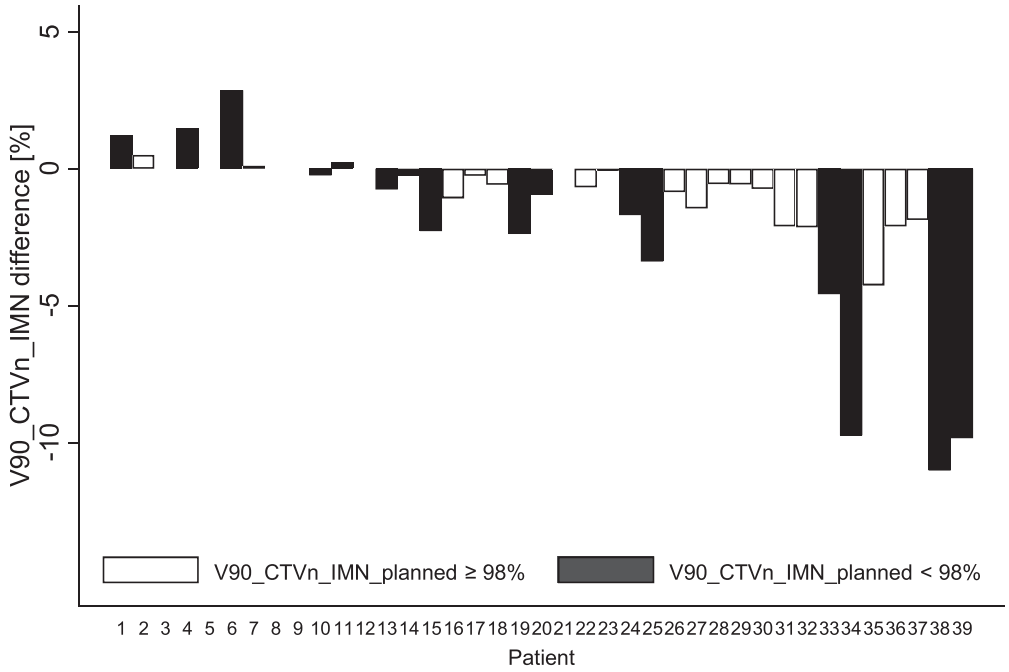

Fig. 5. Difference between delivered and planned V90_CTVn_IMN for patient plans that fulfilled the DBCG guidelines (white) and plans that did not fulfill the guidelines (black). Patients sorted according to mean geometrical errors in field 1 and field 2 from most anterior deviation (patient 1) to most posterior deviation (patient 39).

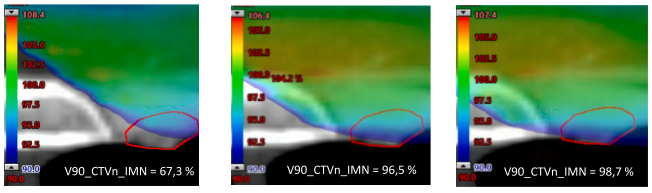

Fig. 6. Dosimetric example for patient 34. The left treatment plan reflects a 6 mm posterior chest wall error (most positive value), the middle treatment plan has no deviation, while the right treatment plan corresponds to a 2 mm anterior chest wall error (most negative value). Color dose wash shows 90% of the prescribed dose. The red structure is the CTVn_IMN. (For interpretation of the references to color in this figure legend, the reader is referred to the web version of this article.)

Furthermore, robustness analysis of the dosimetric impact of setup errors as in Fig. 4 could be performed prior to treatment start to select sensitive treatment plans that would benefit from more frequent cine MV-based monitoring. Volumetric modulated arc therapy (VMAT) may enhance treatment plan robustness, and can also be monitored with cine MV images [28,29]. Detection of the chest wall as well as the heart in the cine MV images of tangential breast fields can be automated [14,21,30] and combined with automated dose reconstruction [31]. This could be used for automated prospective monitoring of the delivered target and OAR doses in BC RT based on daily cine MV imaging. Magnetic resonance imaging might be another strategy to monitor intrafractional movements [32,33].

Using cine MV images, we found that the delivered V90_CTVn_IMN was significantly lower than planned. In 8% of the patients, the V90_CTVn_IMN reduction exceeded 9%. No clinically relevant differences were found for the MLD or MHD. Based on these data our institution plans to implement CBCT for daily IGRT for high-risk BC patients supported by continued cine MV image monitoring.

Funding

The study was supported by the Danish Cancer Society, Aarhus University and DCCC Radiotherapy – The Danish National Research Center for Radiotherapy.

Declaration of Competing Interest

The authors declare that they have no known competing financial interests or personal relationships that could have appeared to influence the work reported in this paper.

Appendix A. Supplementary data

Supplementary data to this article can be found online at https://doi.org/10.1016/j.phro.2023.100470.

References

[1] Whelan TJ, Olivotto IA, Parulekar WR, Ackerman I, Chua BH, Nabid A, et al. Regional nodal irradiation in early-stage breast cancer. N Engl J Med 2015;373:307–16. https://doi.org/10.1056/NEJMoa1415340.
[2] Poortmans PM, Weltens C, Fortpied C, Kirkove C, Peignaux-Casasnovas K, Budach V, et al. Internal mammary and medial supraclavicular lymph node chain irradiation in stage I-III breast cancer (EORTC 22922/10925): 15-year results of a randomised, phase 3 trial. Lancet Oncol 2020;21:1602–10. https://doi.org/10.1016/S1470-2045(20)30472-1.
[3] Thorsen LBJ, Overgaard J, Matthiessen LW, Berg M, Stenbygaard L, Pedersen AN, et al. Internal mammary node irradiation in patients with node-positive early breast cancer: fifteen-year results from the danish breast cancer group internal mammary node study. J Clin Oncol 2022;40:4198–206. https://doi.org/10.1200/JCO.22.00044.
[4] McGale P, Darby SC, Hall P, Adolfsson J, Bengtsson N-O, Bennet AM, et al. Incidence of heart disease in 35,000 women treated with radiotherapy for breast cancer in Denmark and Sweden. Radiother Oncol 2011;100:167–75. https://doi.org/10.1016/j.radonc.2011.06.016.
[5] Cuzick J, Stewart H, Rutqvist L, Houghton J, Edwards R, Redmond C, et al. Cause-specific mortality in long-term survivors of breast cancer who participated in trials of radiotherapy. J Clin Oncol 1994;12:447–53. https://doi.org/10.1200/JCO.1994.12.3.447.
[6] Darby SC, Ewertz M, McGale P, Bennet AM, Blom-Goldman U, Brønnum D, et al. Risk of ischemic heart disease in women after radiotherapy for breast cancer. N Engl J Med 2013;368:987–98. https://doi.org/10.1056/NEJMoa1209825.

[7] Milo MLH, Thorsen LBJ, Johnsen SP, Nielsen KM, Valentin JB, Alsner J, et al. Risk of coronary artery disease after adjuvant radiotherapy in 29,662 early breast cancer patients: a population-based Danish Breast Cancer Group study. Radiother Oncol 2021;157:106–13. https://doi.org/10.1016/j.radonc.2021.01.010.
[8] Thorsen LBJ, Thomsen MS, Berg M, Jensen I, Josipovic M, Overgaard M, et al. CT-planned internal mammary node radiotherapy in the DBCG-IMN study: benefit versus potentially harmful effects. Acta Oncol 2014;53:1027–34. https://doi.org/10.3109/0284186X.2014.925579.
[9] Thorsen LBJ, Thomsen MS, Overgaard M, Overgaard J, Offersen BV. Quality assurance of conventional non-CT-based internal mammary lymph node irradiation in a prospective Danish Breast Cancer Cooperative Group trial: the DBCG-IMN study. Acta Oncol 2013;52:1526–34. https://doi.org/10.3109/0284186X.2013.813643.
[10] Stick LB, Yu J, Maraldo MV, Aznar MC, Pedersen AN, Bentzen SM, et al. Joint estimation of cardiac toxicity and recurrence risks after comprehensive nodal photon versus proton therapy for breast cancer. Int J Radiat Oncol Biol Phys 2017;97:754–61. https://doi.org/10.1016/j.ijrobp.2016.12.008.
[11] Milo MLH, Møller DS, Nyeng TB, Hoffmann L, Nissen HD, Jensen I, et al. Radiation dose to heart and cardiac substructures and risk of coronary artery disease in early breast cancer patients: a DBCG study based on modern radiation therapy techniques. Radiother Oncol 2023;180:109453. https://doi.org/10.1016/j.radonc.2022.109453.
[12] Pedersen AN, Korreman S, Nyström H, Specht L. Breathing adapted radiotherapy of breast cancer: reduction of cardiac and pulmonary doses using voluntary inspiration breath-hold. Radiother Oncol 2004;72:53–60. https://doi.org/10.1016/j.radonc.2004.03.012.
[13] Lutz CM, Poulsen PR, Fledelius W, Offersen BV, Thomsen MS. Setup error and motion during deep inspiration breath-hold breast radiotherapy measured with continuous portal imaging. Acta Oncol 2016;55:193–200. https://doi.org/10.3109/0284186X.2015.1045625.
[14] Vasina EN, Kong N, Greer P, Baeza Ortega J, Kron T, Ludbrook JJ, et al. First clinical experience with real-time portal imaging-based breath-hold monitoring in tangential breast radiotherapy. Phys Imaging Radiat Oncol 2022;24:1–6. https://doi.org/10.1016/j.phro.2022.08.002.
[15] Doebrich M, Downie J, Lehmann J. Continuous breath-hold assessment during breast radiotherapy using portal imaging. Phys Imaging Radiat Oncol 2018;5:64–8. https://doi.org/10.1016/j.phro.2018.02.006.
[16] Conroy L, Guebert A, Smith WL. Technical note: issues related to external marker block placement for deep inspiration breath hold breast radiotherapy. Med Phys 2017;44:37–42. https://doi.org/10.1002/mp.12005.
[17] Hirata K, Yoshimura M, Mukumoto N, Nakamura M, Inoue M, Sasaki M, et al. Three-dimensional intrafractional internal target motions in accelerated partial breast irradiation using three-dimensional conformal external beam radiotherapy. Radiother Oncol 2017;124:118–23. https://doi.org/10.1016/j.radonc.2017.04.023.
[18] Svestad JG, Heydari M, Mikalsen SG, Flote VG, Nordby F, Hellebust TP. Surface-guided positioning eliminates the need for skin markers in radiotherapy of right sided breast cancer: a single center randomized crossover trial. Radiother Oncol 2022;177:46–52. https://doi.org/10.1016/j.radonc.2022.10.017.
[19] Jensen C, Urribarri J, Cail D, Rottmann J, Mishra P, Lingos T, et al. Cine EPID evaluation of two non-commercial techniques for DIBH. Med Phys 2014;41:021730. https://doi.org/10.1118/1.4862835.
[20] Parsons D, Joo M, Iqbal Z, Godley A, Kim N, Spangler A, et al. Stability and reproducibility comparisons between deep inspiration breath-hold techniques for left-sided breast cancer patients: A prospective study. J Appl Clin Med Phys;**24**:e13906. doi:10.1002/acm2.13906.
[21] Nankali S, Hansen R, Worm E, Yates ES, Thomsen MS, Offersen B, et al. Accuracy and potential improvements of surface-guided breast cancer radiotherapy in deep inspiration breath-hold with daily image-guidance. Phys Med Biol 2022;67:195006. https://doi.org/10.1088/1361-6560/ac9109.
[22] Padilla L, Kang H, Washington M, Hasan Y, Chmura SJ, Al-Hallaq H. Assessment of interfractional variation of the breast surface following conventional patient positioning for whole-breast radiotherapy. J Appl Clin Med Phys 2014;15:4921. https://doi.org/10.1120/jacmp.v15i5.4921.
[23] Hong C-S, Ju SG, Choi DH, Han Y, Huh SJ, Park W, et al. Dosimetric effects of intrafractional organ motion in field-in-field technique for whole-breast irradiation. Prog Med Phys 2019;30:65. https://doi.org/10.14316/pmp.2019.30.3.65.
[24] Offersen BV, Boersma LJ, Kirkove C, Hol S, Aznar MC, Sola AB, et al. ESTRO consensus guideline on target volume delineation for elective radiation therapy of early stage breast cancer. Radiother Oncol 2015;114:3–10. https://doi.org/10.1016/j.radonc.2014.11.030.
[25] van Herk M. Errors and margins in radiotherapy. Semin Radiat Oncol 2004;14:52–64. https://doi.org/10.1053/j.semradonc.2003.10.003.
[26] Grantzau T, Thomsen MS, Væth M, Overgaard J. Risk of second primary lung cancer in women after radiotherapy for breast cancer. Radiother Oncol J Eur Soc Ther Radiol Oncol 2014;111:366–73. https://doi.org/10.1016/j.radonc.2014.05.004.
[27] Topolnjak R, Sonke J-J, Nijkamp J, Rasch C, Minkema D, Remeijer P, et al. Breast patient setup error assessment: comparison of electronic portal image devices and cone-beam computed tomography matching results. Int J Radiat Oncol 2010;78:1235–43. https://doi.org/10.1016/j.ijrobp.2009.12.021.
[28] Miura H, Doi Y, Nakao M, Ozawa S, Kenjo M, Nagata Y. Improved treatment robustness of postoperative breast cancer radiotherapy including supraclavicular nodes. Phys Imaging Radiat Oncol 2022;23:153–6. https://doi.org/10.1016/j.phro.2022.08.004.
[29] Carr MA, Gargett M, Stanton C, Zwan B, Byrne HL, Booth JT. A method for beam's eye view breath-hold monitoring during breast volumetric modulated arc therapy. Phys Imaging Radiat Oncol 2023;25:100419. https://doi.org/10.1016/j.phro.2023.100419.
[30] Poulsen PR, Thomsen MS, Hansen R, Worm E, Spejlborg H, Offersen B. Fully automated detection of heart irradiation in cine MV images acquired during breast cancer radiotherapy. Radiother Oncol 2020;152:189–95. https://doi.org/10.1016/j.radonc.2019.11.006.
[31] Andresen S, Muurholm C, Skouboe S, Spejlborg H, Offersen B, Poulsen P. Fully automated heart dose calculation from cine MV images recorded during breast cancer treatments. Radiother Oncol 2020;152:114–5. https://doi.org/10.1016/S0167-8140(21)00248-6.
[32] Groot Koerkamp ML, van den Bongard HJGD, Philippens MEP, van der Leij F, Mandija S, Houweling AC. Intrafraction motion during radiotherapy of breast tumor, breast tumor bed, and individual axillary lymph nodes on cine magnetic resonance imaging. Phys Imaging Radiat Oncol 2022;23:74–9. https://doi.org/10.1016/j.phro.2022.06.015.
[33] Habatsch M, Schneider M, Requardt M, Doussin S. Movement assessment of breast and organ-at-risks using free-breathing, self-gating 4D magnetic resonance imaging workflow for breast cancer radiation therapy. Phys Imaging Radiat Oncol 2022;22:111–4. https://doi.org/10.1016/j.phro.2022.05.007.